

Study of decay properties of Ba to Nd nuclei ($A \sim 160$) relevant to the formation of the r-process rare-earth peak

M. Pallàs^{1*}, A. Tarifeño-Saldivia^{2,1†}, G. G. Kiss³, J. L. Tain², A. Tolosa-Delgado^{5,2}, A. Vitéz-Sveiczer^{3,4}, F. Calviño¹, J. Agramunt², P. Aguilera⁶, A. Algora², J. M. Allmond⁷, H. Baba⁸, N. T. Brewer^{9,7}, R. Caballero-Folch¹⁰, P. J. Coleman-Smith¹¹, G. Cortes¹, T. Davinson¹², I. Dillmann^{10,13}, C. Domingo-Pardo², A. Estrade¹⁴, N. Fukuda⁸, S. Go^{15,16}, C. J. Griffin¹⁰, R. K. Grzywacz^{9,7}, O. Hall¹², L. J. Harkness-Brennan¹⁷, T. Isobe⁸, D. Kahl¹², T. T. King⁹, A. Korgul¹⁸, S. Kovács⁴, S. Kubono⁸, M. Labiche¹¹, J. Liu¹⁹, M. Madurga⁹, K. Miernik¹⁸, F. Molina⁶, N. Mont-Geli¹, A. I. Morales², E. Nácher², A. Navarro¹, N. Nepal⁸, S. Nishimura⁸, M. Piersa-Silkowska¹⁸, V. Phong⁸, B. C. Rasco^{9,7}, J. Romero-Barrientos⁶, B. Rubio², K. P. Rykaczewski⁷, Y. Saito^{10,20}, H. Sakurai⁸, Y. Shimizu⁸, M. Singh⁹, T. Sumikama⁸, H. Suzuki⁸, T. N. Szegedi³, H. Takeda⁸, K. Wang¹⁴, M. Wolińska-Cichocka²¹, P. J. Woods¹², and R. Yokoyama¹⁶ for the BRIKEN collaboration²²

¹Institut de Tècniques Energètiques (INTE), Universitat Politècnica de Catalunya (UPC), 08028 Barcelona, Spain.

²Instituto de Física Corpuscular (IFIC), CSIC-UV, E-46980 Paterna, Spain.

³Institute for Nuclear Research (ATOMKI), 4026 Debrecen, Bem tér 18/c, Hungary.

⁴University of Debrecen, 4032 Debrecen, Egyetem tér 1, Hungary.

⁵Department of Physics, University of Jyväskylä, Finland.

⁶Centro de Investigación en Física Nuclear y Espectroscopía de Neutrones (CEFNEN). Comisión Chilena de Energía Nuclear, Nueva Bilbao 12501, Las Condes, Santiago-Chile.

⁷Physics Division, Oak Ridge National Laboratory, Oak Ridge, TN 37830, USA.

⁸RIKEN Nishina Center, 2-1 Hirosawa, Wako, Saitama 351-0198, Japan.

⁹Department of Physics and Astronomy, University of Tennessee, Knoxville, Tennessee 37996, USA.

¹⁰TRIUMF, 4004 Wesbrook Mall, Vancouver, BC V6T 2A3, Canada.

¹¹STFC Daresbury Laboratory, Daresbury, Warrington WA4 4AD, United Kingdom.

¹²School of Physics and Astronomy, The University of Edinburgh, Edinburgh EH9 3FD, United Kingdom.

¹³Department of Physics and Astronomy, University of Victoria, Victoria, BC V8P 5C2, Canada.

¹⁴Central Michigan University, Mt. Pleasant, MI 48859, USA.

¹⁵Department of Physics, Kyushu University, 744 Motooka, Fukuoka 819-0395, Japan.

¹⁶Center for Nuclear Study, The University of Tokyo, 2-1 Hirosawa, Wako, Saitama 351-0106, Japan.

¹⁷Department of Physics, University of Liverpool, Liverpool L69 7ZE, United Kingdom.

¹⁸Faculty of Physics, University of Warsaw, 02-093 Warsaw, Poland.

¹⁹Department of Physics, the University of Hong Kong, Pokfulam Road, Hong Kong.

²⁰Department of Physics and Astronomy, The University of British Columbia, Vancouver BC V6T 1Z1, Canada.

²¹Heavy Ion Laboratory, University of Warsaw, Pasteura 5A, 02-093 Warsaw, Poland.

²²www.wiki.ed.ac.uk/display/BRIKEN/Home

[†]atarisal@ific.uv.es

*max.pallas@upc.edu

Abstract. Half-lives ($T_{1/2}$) of exotic neutron-rich isotopes of Ba, La, Ce, Pr, and Nd were measured at the RIKEN Nishina Center. The experimental setup consisted of the BigRIPS in-flight separator for ion selection identification, the Advance Implantation Detector Array (AIDA) for ions and β detection, and the BRIKEN detector for neutron counting. Using this setup, 4 new $T_{1/2}$ have been measured for the first time, and 38 $T_{1/2}$ have been remeasured with improved precision in several cases. These new experimental data should help to constrain theoretical models for calculations of $T_{1/2}$. The status of the experimental analysis and preliminary results are provided in this contribution.

1 Introduction

Rapid neutron capture in explosive stellar scenarios (the r-process) produces almost half of the nuclei heavier than iron. For nuclear masses $A > 100$, there are two main peaks in the r-process solar system element abundances, located at $A \sim 130$ and $A \sim 195$, which are associated with the neutron shell closure at $N = 82$ and $N = 126$ affecting the r-process path during the $(n, \gamma) \leftrightarrow (\gamma, n)$ equilibrium. The Rare-Earth Peak (REP), on the other hand, is a small but distinct peak around mass $A \sim 160$ that results from the freeze-out in the final stages of neutron exhaustion. Thus, the formation of the REP may provide a unique probe for examining the late-time conditions at the r-process site. According to theoretical models and sensitivity studies, the half-lives ($T_{1/2}$) and beta-delayed neutron emission probabilities (P_{xn}) of very neutron-rich nuclei, in the mass region $A \sim 160$ for $55 \leq Z \leq 64$, are critical for the formation of the REP [1, 2].

The BRIKEN project [3, 5] has been in operation from 2016 to 2021 at the Radioactive Isotope Beam Factory (RIBF) in the RIKEN Nishina Center. This collaboration has carried out a thorough measurement program of the β -decay properties of the most neutron-rich nuclei experimentally available. The BRIKEN REP proposal focused on measurements from Ba to Gd ($A \sim 160$) at the RIKEN Nishina Center. The entire REP proposal comprised three experimental campaigns. Recently, a first publication has been released with the experimental results for Pm to Gd species, including also an assessment of their astrophysical significance [6]. The data analysis for Ba to Nd species is the main focus of this work. We report preliminary results of $T_{1/2}$ for nuclei in the neutron-rich region from Ba to Nd. Results on P_{xn} values will be presented at later stage. The experimental setup and status of the data analysis on this region are also discussed.

2 Experimental setup

The exotic neutron-rich isotopes were produced at RIKEN Nishina Center using a 60 pnA ^{238}U primary beam, with an energy of 345 MeV/nucleon, bombarding a 5 mm thick ^9Be target. The fragments from the collision are selected by BigRIPS in-flight separator and guided to the experimental area through the Zero-Degree Spectrometer (ZDS) [7]. Each ion reaching the experimental area was identified by measuring its atomic charge (Z), and its mass-to-charge ratio (A/Q). Identified ions were implanted in the Advanced Implantation Detector Array (AIDA) [10]. AIDA consists of a stack of six silicon Double-Sided Strip Detectors (DSSD) separated by 10 mm gaps. Each DSSD has a thickness of 1 mm, and 128 strips per side. The strips on the two sides are perpendicular to each other, forming a 16384-pixel silicon detector. This configuration offers a high spatial resolution, allowing the reconstruction of implant and β -decay events.

The BRIKEN neutron counter [11] was placed surrounding AIDA in order to detect directly the β -delayed neutrons. It consisted of an array of 140 ^3He -filled proportional tubes embedded in a 90 cm x 90 cm x 75 cm High-

Density PolyEthylene (HDPE) moderator, thus providing an almost 4π neutron detector. Neutron moderation is required in order to achieve high overall detection efficiencies thanks to the large cross section for thermal neutrons in the reaction $n_{th} + ^3\text{He} \rightarrow ^3\text{H} + p$. The HDPE block has a central hole of 11.6 cm x 11.6 cm where AIDA is inserted. It also has additional holes at both sides, where two CLARION-type clover detectors are placed to offer γ detection capabilities [11]. Figure 1 provides a scheme and a picture of the BRIKEN setup. The neutron efficiency of the BRIKEN detector has been calculated by Monte Carlo (MC) simulations, it is independent of the neutron energy up to 1 MeV, it has a nominal value of 68.6% and shows a smooth decrease at higher energies. The MC calculations of the neutron efficiency have been validated experimentally using a ^{252}Cf neutron source, obtaining good agreement between the measurement and simulations [12]. The rawdata is collected by three independent data acquisition systems (DAQs) from BigRIPS, AIDA, and BRIKEN detectors. For this reason, a synchronization signal has been fed into each DAQ, thus producing a common timestamp reference and allowing the reconstruction offline of the identified implant-decay events.

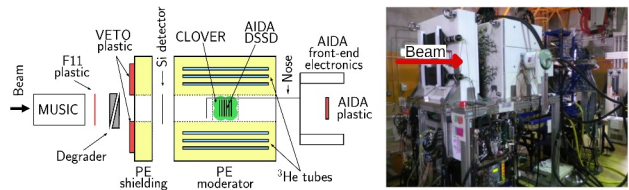


Figure 1. Schematic drawing and photograph of the BRIKEN setup.

3 Data analysis methodology

The main goal of this experiment is to measure half-lives ($T_{1/2}$) and β -delayed neutron branchings (P_{xn}) associated with the decay of the implanted ions. To this end, we took advantage of the good spatial and time resolution of our setup in order to build spatial and temporal correlations. Thus, for each identified implanted isotope, we build a correlation between implants and beta events (H_{β} histogram). This histogram stores the time difference between an implant and all the β events that took place in the same position within a defined time window. Using this procedure, the truly correlated decays will form a decay curve clearly distinguishable from the background produced by uncorrelated events. In the case of the β -delayed neutrons, we built the implant- β -neutron correlation ($H_{\beta xn}$ histograms). These histograms are constructed in a similar way as the H_{β} , but they require the detection of x neutrons ($x:1, 2, \dots$) in the BRIKEN counter within a fixed time window with respect to the β detection. The last step to obtain the physical magnitudes of interest, namely $T_{1/2}$ and P_{xn} , is to fit all histograms using the solution of the Bateman equations ([4]), for all the decay descendants [5]. We used the

generic form of the proposed solution, which in our particular case simplifies to:

$$N_k(t) = N_1 \prod_{i=1}^{k-1} (b_{i,i+1} \lambda_i) \times \left(\sum_{i=1}^k \frac{e^{\lambda_i t}}{\prod_{j=1 \neq i}^k (\lambda_j - \lambda_i)} \right) \quad (1)$$

The initial number of implanted parent nuclei is $N_1 = N_1(t = 0)$, the decay constant is $\lambda = \ln 2 / T_{1/2}$, and the number of k-type nuclei in a given decay path at time t is $N_k(t)$. The branching ratio $b_{i,i+1}$ in the decay chain from nucleus i to nucleus $i + 1$ defines the decay path. The backward-time distribution was used to calculate the correlated accidental background. The fit procedure is performed simultaneously on all histograms in order to get self-consistency on the fit parameters [5]. As an example of the data analysis, the decay path and the fit are shown in Figures 2 and 3, respectively, for the decay of ^{153}La .

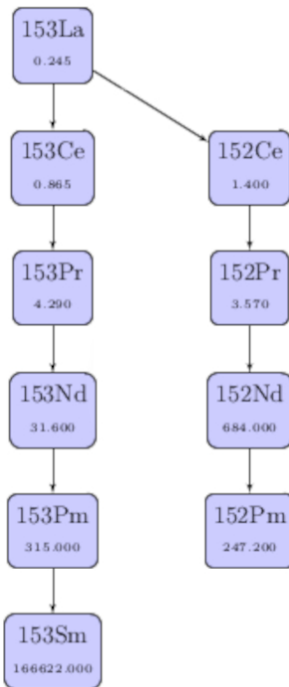


Figure 2. Diagram depicting the various decay paths for ^{153}La disintegration. Each number below a nucleus is the $T_{1/2}$ used as input.

4 Preliminary results and discussion

The Particle IDentification (PID) matrix obtained with AIDA for the REP-BRIKEN 2018 dataset is presented on the top panel of Figure 4. The bottom one shows the projection of the PID matrix on the A/Q axis for the Pr isotopes. For the less exotic region ($A < 159$) the achieved A/Q resolution is good enough — typically less than 0.05% — to ensure a good separation of fully-stripped and H-like ions. The preliminary results of the measured $T_{1/2}$ in this work are presented in Figure 5. At least 4 new half-lives in the La-Nd region are obtained from the BRIKEN REP experiment: ^{157}La , ^{159}Ce , ^{161}Pr , and

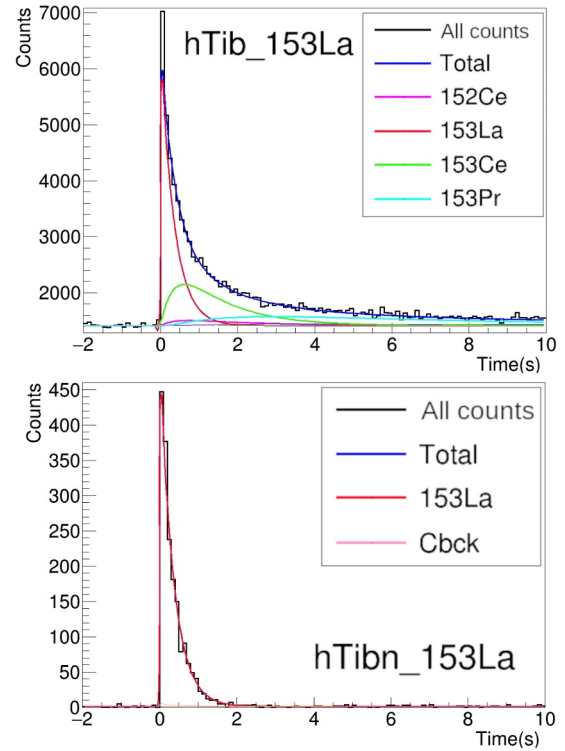


Figure 3. Fit to implant- β time correlation histograms (top) and implant- β -1n time correlation histograms (bottom) for ^{153}La . All the decay chain from Figure 2 was used to run the fit, but in this figure only the isotopes with a significant contribution are included.

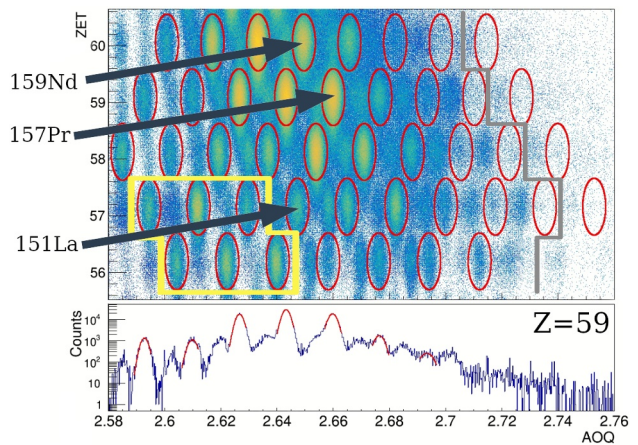


Figure 4. Identification plot of the REP-BRIKEN 2018 experiment. Each red circumference corresponds to an identified isotope. The grey line indicates the limit of previously measured $T_{1/2}$ [9]. Yellow box highlights previously measured P_{1n} values. The bottom panel depicts the projection of the PID matrix on the A/Q axis for the Pr isotopes.

^{163}Nd . The determination of the final values and uncertainties for these new half-lives is still in progress. We expect to achieve a further reduction of the charge-state contamination in the most exotic region by improving the particle identification. This is being implemented based on the correlation between A/Q and the total ion energy

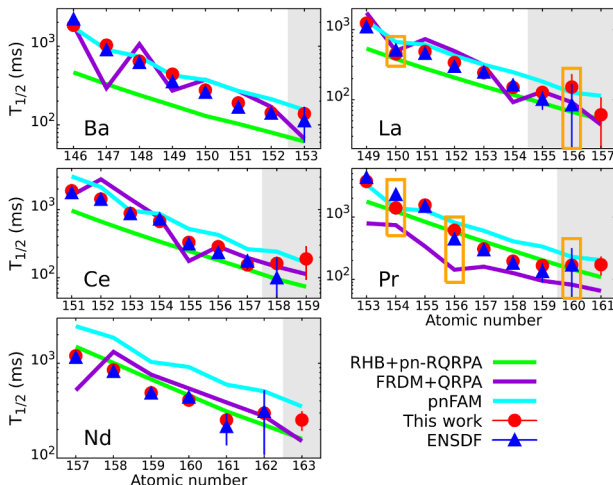


Figure 5. Preliminary results for $T_{1/2}$ from this work (in red), previous measurements (in blue). These results are compared to three theoretical models: RHB+pn-RQRPA [13] (in green), FRDM+QRPA [14] (in purple), and pnFAM [15] (in light-blue). The grey region highlights expected improvements on the determination of half-lives by the end of the data analysis. Orange boxes indicate potential isomer contribution [16].

loss measured in AIDA. Moreover, in the less exotic region, a total of 38 $T_{1/2}$ have been remeasured with improved accuracy in several cases. Furthermore, in Figure 5, our preliminary results are compared with evaluated nuclear data from the ENSDF and some recent theoretical predictions: Relativistic Hartree-Bogoliubov plus proton-neutron Relativistic Quasi-Particle Random-Phase Approximation (RHB+pn-RQRPA, 2016) [13], Finite-Range Droplet-Model mass formula (2012) plus Quasiparticle-Random-Phase Approximation (FRDM+QRPA, 2018) [14], and the proton-neutron Finite Amplitude Method (pnFAM, 2020) [15]. Compared with the evaluated nuclear data, our preliminary results are consistent within a 3σ error band. The only significant differences arise for isotopes with potential isomeric states. We still need to conduct an evaluation of the contribution to the decay of the potential isomer. Concerning the comparison with theoretical models, the overall trend for all half-lives predictions is confirmed by our data. The RHB+pn-RQRPA provides estimates close to experiment for Nd and Pr nuclei and underestimates the values for Ba, La and Ce. However, this model tends to underestimate Ce, La, and Ba nuclei. For the case of the FRDM+QRPA model, there is a clear underprediction of experimental values for Pr isotopes and the significant odd-even staggering predicted for the region $56 \leq Z \leq 60$ is not reproduced neither by the

evaluated experimental data nor by our new data. This observation is also in agreement with the results for the region $50 \leq Z \leq 57$ [17]. Finally, the pnFAM model shows a tendency to overestimate the half-lives, which is particularly noticeable for the neutron rich isotopes in general and for all Nd isotopes measured in this work.

5 Acknowledgment

This work has been supported by the Spanish Ministerio de Economía y Competitividad under Grants. FPA2014-52823-C2-1-P, FPA2014-52823-C2-2-P, FPA2017-83946-C2-1-P, FPA2017-83946-C2-2-P and grants from Ministerio de Ciencia e Innovación PID2019-104714GB-C21, PID2019-104714GB-C22. Supported by Generalitat Valenciana regional grant PROMETEO/2019/007. Supported by European Union FEDER funds. It also has been supported by NKFH (NN128072).

References

- [1] A. Arcones and G. Martínez Pinedo, *Phys. Rev. C* **83**, 045809 (2011).
- [2] M. R. Mumpower, et al., *Phys. Rev. C* **85**, 045801 (2012).
- [3] J. L. Tain, et al., *Acta physica polonica B* **49**(03), 417 – 428 (2018).
- [4] H. Bateman, et al., *Proc. Cambridge Philos* **10** 5, 423 – 427 (1910).
- [5] A. Tolosa-Delgado, et al., *NIM A* **925**, 133 – 147 (2019).
- [6] G. G. Kiss, et al., *The Astrophysical Journal* **936** 2, 107 (2022).
- [7] T. Kubo, et al., *Prog. Theor. Exp. Phys.* 03C002 (2012).
- [8] N. Fukuda, et al., *NIM B*, 317 – 323 (2013).
- [9] J. Wu, et al., *Phys. Rev. Lett.* **118** 7 072701 (2017).
- [10] C. J. Griffin, et al., *Jap. Phys. Soc. Conf. Proc.* **14**, 020622 (2017).
- [11] A. Tarifeño-Saldivia, et al., *J. Instrum.* **12**(04):P04006 (2017).
- [12] M. Pallas, et al., ArXiv:2204.13379 (2022).
- [13] T. Marketin, et al., *Phys. Rev. C* **93** 2 025805 (2016).
- [14] P. Möller, et al., *At. Data Nucl. Data* **125** 1 – 192 (2019).
- [15] E. M. Ney, et al., *Phys. Rev. C* **102** 3 034326 (2020).
- [16] Nndc.bnl.gov. 2022. Experimental Un-evaluated Nuclear Data List. Available at: <<https://www.nndc.bnl.gov/ensdf/xndl/>>.
- [17] J. Wu et al., *Phys. Rev. C* **101**, 042801(R) (2020).